Elsevier Editorial System(tm) for Fuel
Manuscript Draft

Manuscript Number: JFUE-D-17-01687R1

Title: Insights on the combustion mechanism of ethanol and n-hexane in honeycomb monolithic type catalysts: influence of the amount and nature of Mn-Cu mixed oxide

Article Type: Research paper

Keywords: Manganese-Copper mixed oxide; Cordierite; Ethanol; n-hexane; VOC oxidation

Corresponding Author: Dr. Maria Roxana Morales, Dr

Corresponding Author's Institution: Universidad Nacional de San Luis

First Author: Maria Roxana Morales, Dr

Order of Authors: Maria Roxana Morales, Dr; Maria Pilar Yeste, Dr.; Hilario Vidal Muños, Dr.; Jose Manuel Gatica Casas, Dr.; Luis E Cadus, Dr.

Abstract: Mn-Cu mixed oxides were deposited by ultrasonic impregnation on ceramic honeycomb monoliths. Its catalytic performance was evaluated in the combustion of ethanol and n-hexane, VOC molecules of different chemical nature. The catalysts were characterized by N2 physisorption, SEM-EDS, XRD, X-ray fluorescence, XPS, TPR, TPD-O2 and OSC measurements. It was observed that the catalyst with the lowest content of Mn-Cu phase was the most active in the combustion of ethanol. This was attributed to the higher content of Mn4+ and the increase of lattice oxygen mobility, which would favor a Mars-van Krevelen type mechanism. The catalyst with a medium content of Mn-Cu, proved to be the most active in the combustion of n-hexane. This was associated with a high content of oxygen vacancies and easy availability of oxygen adsorbed on the surface, promoting the combustion of n-hexane, possibly through a Rideal-Eley type mechanism. The catalyst with the highest content of the Mn-Cu phase showed low activity in combustion of ethanol and n-hexane, which was attributed to a higher crystallinity of the Mn-Cu phases generated.

CONICET UNSL

I N T E Q U I

San Luis, Argentina, May 05, 2017.

Dear Editor

I am pleased to submit the manuscript entitled "***Insights on the combustion mechanism of ethanol and n-hexane in honeycomb monolithic type catalysts: influence of the amount and nature of Mn-Cu mixed oxide"*** by María Roxana Morales, M. Pilar Yeste, Hilario Vidal, José M. Gatica and Luis E. Cadús, to be considered for publication in ***Fuel*** as a research paper.

This research focuses on the optimization of the synthesis of catalysts, destined to the combustion of VOCs. The different arrangements of surface catalytic phases achieved have allowed to infer in the possible mechanisms of oxygen supply in the oxidation of two molecules of VOCs with different chemical nature. This research is clearly catalytic and environmental.

The manuscript has been prepared in compliance with the Ethics in Publishing Policy as described in the Guide for Authors. The manuscript is not a re-submission.

Yours Faithfully,



Dr. Maria Roxana Morales

INTEQUI (UNSL – CONICET)

5700 San Luis - Argentina

Tel/Fax: 0054(0)266-4520300 int. 1319

E-mail: mrmorale14@gmail.com

***Detailed Response to Reviewers**

Manuscript JFUE-D-17-01687

María Roxana Morales et al: Insights on the combustion mechanism of ethanol and n-hexane in honeycomb monolithic type catalysts: influence of the amount and nature of Mn-Cu mixed oxide.

Dear Editor,

Please find below our answers to the comments of the referees. They appear one by one after each inquiry also included in blue. Please notice that the numbers of lines indicated in the response (below) correspond to the initial submitted manuscript. In the revised version, the sentences added or modified appear with slightly different line numeration.

Reviewer #1: The work is focused on the influence of the amount and nature of Mn-Cu mixed oxide for the combustion of ethanol and n-hexane in honeycomb monolithic type catalysts. The characterization is detailed, with particular care to the identification of the different Mn-Cu contents, oxygen species, catalyst properties, and combustion mechanism of VOCs. I think any attempt to control the emissions of pollutants should be encouraged. Furthermore, the topic is state-of the-art and pertinent to the scopes of the journal. The text is also organized well. I suggest that it can be published in the journal of FUEL, but it should be revised as following.

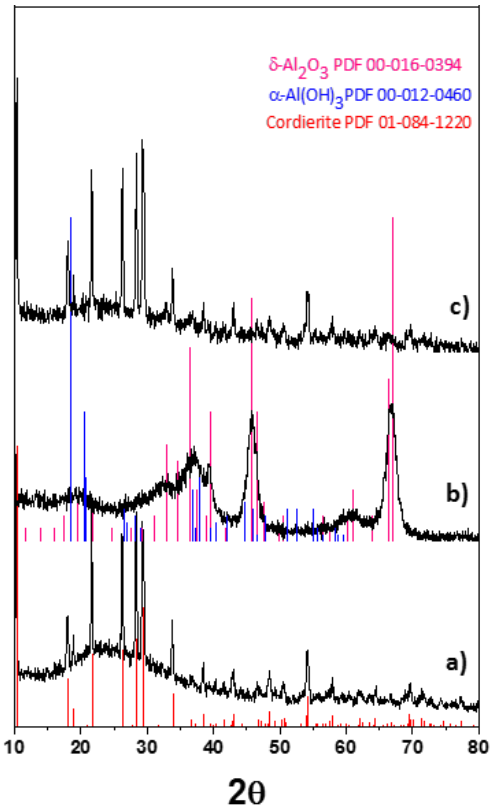
1. In the combustion of ethanol and n-hexane, had the authors detected byproducts? The carbon balance of the reaction should be given.

In Section 3.4, from line 324 to line 327, it is mentioned that acetaldehyde was detected as byproduct of an incomplete oxidation, in the combustion of ethanol, at low temperatures or conversion levels. The carbon balance was closed at ±5% for both reactions. In the n-hexane reaction, no by-products were detected as indicated (lines 345-347).

In the text, in Section 3.4, line 324 (Line 327 now), the following sentence is added: …."The carbon balance was closed at ±5% for both reactions."…..

2. In the Figure 2, the three XRD patterns were displayed separately. I think that the three pictures should be put together into one just as Figure 3.

As suggested by the Reviewer, Figure 2 was modified, and the three diffractograms were put together into only one image.



3. In the section 3.2, the author calmed "From the (Mn + Cu)/Al ratio the dispersion degree of the Mn-Cu phase on the alumina could be estimated. A1C2 showed the highest dispersion, while A1C1 showed the lowest one (Table 2)". But from Table 2, one can that the Mn/(Mn+Cu) ratios over the A1C1, A1C2, and A2C2 samples are 0.86, 0.88, and 0.84". The numerical value is so close to be insufficiency to give the conclusion, only if the test error is small enough.

In Section 3.2, the dispersion degree is reported as the (Mn + Cu)/Al ratio, whose values are in Table 2, in column 5, being A1C1 = 0.12, A1C2 = 0.32 and A2C2 = 0.21. As can be seen, for this (Mn + Cu)/Al relation the values are significantly different from each other (lines 234 to 235).

The values corresponding to A1C1 = 0.86, A1C2 = 0.88 and A2C2 = 0.84 correspond to the Mn/(Mn + Cu) relation. In the literature [Xingyi W, Qian K, Dao L.

Catalytic combustion of chlorobenzene over MnOx–CeO_2 mixed oxide catalysts, Appl. Catal. B 2009; 86:166-175], this relationship has been associated with a process, in which electrons from the oxygen are transferred to the manganese, leading to the formation of electrophilic oxygen species. This is detailed on lines 221 to 226.

In the text, in Section 3.2, line 225 (Line 227 now), the following sentence is added: …." As can be seen in Table 2 for the (Mn/Mn+Cu) ratio, the catalyst …….

4. In the section 3.3, the author wrote "If the areas are expressed as the H2 consumption per gram of Mn-Cu phase, it can be seen in Table 4 that the A1C1 catalyst has a H2 consumption that is approximately four times that shown by the rest of the catalysts, which is consistent with data obtained by XPS". As we known that the XPS can give the information about the surface of the catalyst, whereas the TPR experiment results are determined by the bulk properties of the sample. Therefore, the results are difficult to be compared.

We totally agree that both techniques provided complementary information: one related with surface and the other with bulk of the samples. Therefore, one must be careful when comparing the respective results. In any case, the obtained data suggest that the most external surface of our catalysts reflects the manganese composition of the bulk. At this respect, we have decided to edit the manuscript to better clarify this point.

In the text, in Section 3.3, line 275 to 276 (Line 275 to 278 now), the following sentence is added: … …. by XPS as this technique indicated that A1C1 sample is the one having highest Mn^{4+} content. The combination of both results also suggest that the external surface composition resembles that of the bulk. The consumption …

Reviewer #2: This works deals about the elimination of two VOCs using as catalysts honeycomb monolithic materials with added MnCu oxides. The work is reasonably clear and, as far as I know, the same composition, preparation procedure and nature of VOCs employed has not been reported before. The catalytic results obtained are not notable as full conversion is obtained at temperatures of 250ºC for ethanol oxidation and higher for n-hexane. The compounds chosen (ethanol and hexane) present high reactivity and usually not high reaction temperatures are required.

The mass of the catalyst defines the values of the total conversion temperatures of the different VOCs. The catalyst load ranges from 0.024 mg (A1C1) to 0.066 mg (A2C2), which is an order of magnitude lower than the one reported in the literature, in which, for monoliths of equal size the catalyst load is approximately 0.3 mg. Therefore, it is remarkable to reach these temperatures for the complete combustion. In a future scaling of the catalyst, the energy expenditure required to reach this combustion temperature will be entirely compensated by the economy in the type of metals constituting the catalyst and mainly in the catalyst load mass.

1. I miss the results of representative reference samples. In the three catalysts tested Mn and Cu are used (only 3 catalysts in total). What about similar catalysts with only Cu or only Mn? This way we could check if the Mn-Cu mixture enhances the reactivity compared to the pure samples and then a synergetic effect is observed. As we do not have that reference we do not know if the addition of a second element is worthy.

The research group has a wide knowledge in the Mn-Cu mixed system. It has been studied in both mass form and supported in different supports [Morales MR, Barbero BP, Cadus LE. Total oxidation of ethanol and propane over Mn-Cu mixed oxide catalysts. Appl. Catal. B: Environmental 2006;67:229-236. Morales MR, Barbero BP, Cadus LE. Evaluation and characterization of Mn-Cu mixed oxide catalyst for ethanol total oxidation: Influence of copper content. Fuel 2008;87:1177-1186. Morales MR, Barbero BP, Cadus LE. MnCu catalyst deposited on metallic monoliths for total oxidation of volatile organic compounds. Catal. Lett. 2011;141:1598-1607]. It has been shown that the activity of Mn-Cu mixed systems is higher to those of the simple oxides, especially in the case of the copper. Manganese has shown a good activity but lower than the one of the mixed system. The catalytic performance of the mixed system has been related to the formation of a mixed oxide where Mn^{4+}-Mn^{3+} and Cu^{1+}-Cu^{2+} redox pairs are involved. Currently,

we are writing another publication where it is shown that the supported pure Mn oxide shows good activity, but it is very unstable under reaction conditions.

2. It is said in the text that the OSC gives a thermodynamic limit of the process. Please, explain carefully that, because this statement is not thoroughly true.

In the TWC catalysts characterization context, the oxygen storage capacity (OSC) measurements have been used extensively. At least formally, most of authors differentiate dynamic (or fast) OSC, which is related to the most readily available oxygen atoms, and thermodynamic (or total, maximum, ultimate) OSC, which is the total oxygen available from the catalyst under specific conditions. In our investigation, we measured the oxygen volumetric consumption for samples previously reduced at 350°C and evacuated at 400°C. Take into account that we used a Micromeritics ASAP 2020C automatized analyser, which allows the obtaining of data with a highly demanding equilibrium versus time criterion. So we decided to use the term "thermodynamic limit". Nevertheless, we understand the point arisen by the referee and we decided to modify the text in order to better justify the inclusion of this type of experiments.

In the text, in Section 3.3, line 278 to 280 (Line 280 to 283 now), the following sentence is added:……"Taking into account that the TPR investigation only provides information about the reduction of the samples under dynamic conditions with increasing temperatures, we decided to perform also ultimate OSC experiments which would give a good approximation for the thermodynamic limit of the oxygen release process for samples previously reduced at 350 ºC and evacuated at 400 °C."

3. Authors explain some results considering different reaction mechanisms. I do not deny that this can be true. However, there are not evidences in the article for that. Authors should be more prudent in this aspect by using "we suggest that.. it is possible that... it could be...". This is not a mechanistic study and there are not evidences. Please, modify.

As requested by the reviewer, in the text were modified the expressions referring to the possibility of the different mechanisms by which the oxidation of the two VOCs is carried out.

In the text, the following lines were modified: **lines 16, 20, 378-379 (382-384 now), 383-384 (387-388 now), 406-407 (410-411 now), 411-412 (415-416 now).**

4. It does not remain clear the feed used in the catalytic reactions. It is much more reproducible by other authors if the feed is given as hexane(ethanol)/O2/N2 (or He) = // in mol%. Please, do it.

In Section 2.3, line 131 to 132 (Lines 130 to 132 now), the composition of the feed stream of each VOC was written in the way the reviewer requested:

"……..The reacting stream was 500 cm^3 min^{-1} with a composition of C2H5OH:O_2:N_2 = 0.25:20.94:78.81 for ethanol and C6H14:O_2:N_2 = 0.14:20.97:78:89 for n-hexane……."

5. In ethanol oxidation acetaldehyde has been detected. Please, provide more info in terms of selectivity or yield to acetaldehyde with the temperature.

Since the carbon balance closes at ±5% (reported to reviewer 1) and no other intermediate compound is detected, it is unnecessary to report the performance of the only intermediary. At low temperatures, the selectivity to acetaldehyde is 98 ± 2%, while at 100% conversion the selectivity to acetaldehyde is 4 ± 2%.

6. There is not data about the temperature at which 100% hexane conversion has been obtained. Please, supply this info. In Fig 9 the highest conversion shown is ca 80%. This conversion is given at 290ºC whereas the activation temperature of these materials is 500ºC. There is a big gap to study reaction temperatures higher than 290ºC.

The temperatures reported for the conversion of n-hexane were selected to compare conversions and intrinsic activity in the temperature range of ethanol conversion. The 100% conversion of n-hexane was achieved at 345°C for A1C1, 327°C for A1C2 and 340°C for A2C2.

In section 3.4, line 347 (Line 350 to 351 now), the following text was added: "Total conversion of n-hexane was achieved at 345°C (A1C1), 327°C (A1C2) and 340°C (A2C2)".

7. Please, give details about the way the figure 10 has been represented. How have the authors determined T50 and T90 after different times? One plateau and then the temperature was decreased until room temperature and then a ramp again until 400ºC? What is the duration of that ramp? Please, supply info about the experimental part of these stability experiments.

Catalysts were evaluated by taking measurements every 25°C, and the complete light-off curves require approximately 8 h of evaluation. When the 100% conversion

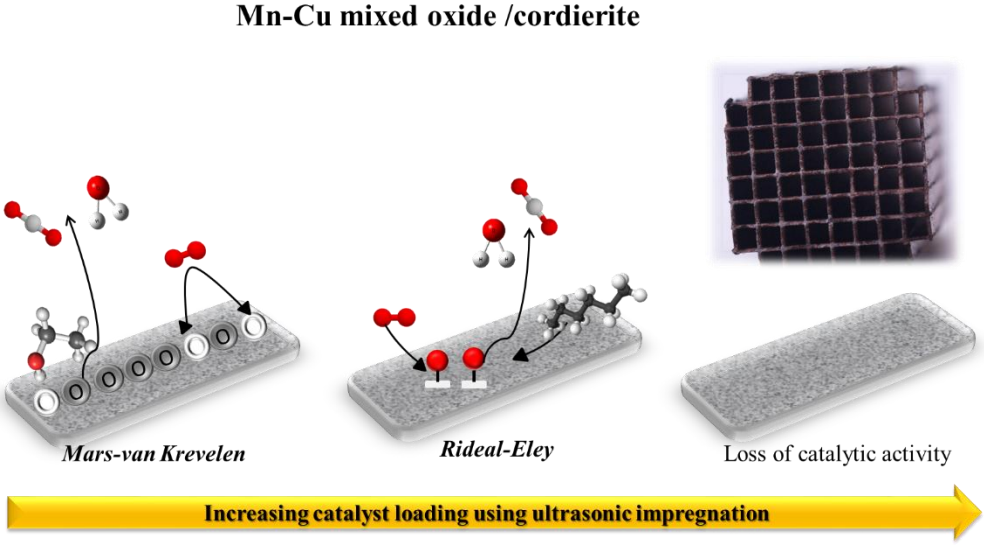
is reached, the reaction is maintained at that conversion level for 12 h. Then, it is cooled at room temperature in a sealed atmosphere and evaluated again by taking measurements every 25°C until 100% conversion is reached, then maintained at 100% conversion for 12 h, then cooled at room temperature under a sealed atmosphere and, finally, taking again every 25°C up to 100% conversion. The T_{50} and T_{90} data were extrapolated from the light-off curves obtained at each time.

In the text in Section 2.3, line 143 to 145 (Line 143 to 148 now), the following text was added:….. "Conversion measurements were taken every 25°C until reaching 100% conversion. When this conversion level was reached, the temperature was increased to 350°C and held for 12 h. Then the temperature was decreased to room temperature and again the light-off curve was lifted. This was repeated once again, obtaining 3 complete light-off curves. T_{50} values (50% conversion temperatures) and T_{90} (90% conversion temperature) were obtained from the light-off curves at different times, i.e., 8 h, 20 h and 40h (Figure 10).”…….

HIGHLIGHTS

- Mn-Cu catalysts deposited on ceramic monoliths using ultrasonic impregnation.
- Mn-Cu catalysts evaluated in the total oxidation of volatile organic compounds of different chemical nature.
- Effect of alumina and active phase loads in the catalytic activity and mechanisms of oxygen supply.

GRAPHICAL ABSTRACT



*Manuscript
Click here to view linked References

Insights on the combustion mechanism of ethanol and n-hexane in honeycomb monolithic type catalysts: influence of the amount and nature of Mn-Cu mixed oxide

Maria R. Morales[a]*, M. Pilar Yeste[b], Hilario Vidal[b], José M. Gatica[b], Luis E. Cadus[a]

[a] *Instituto de Investigaciones en Tecnología Química (INTEQUI), Universidad Nacional de San Luis - CONICET, San Luis, Argentina. E-mail: mrmorale14@gmail.com – luiscadus@gmail.com*

[b] *Departamento de Ciencia de los Materiales e Ingeniería Metalúrgica y Química Inorgánica, Universidad de Cádiz, 11510 Puerto Real, España. E-mail: pili.yeste@uca.es – hilario.vidal@uca.es – josemanuel.gatica@uca.es*

** E-mail: mrmorale14@gmail.com*

ABSTRACT

Mn-Cu mixed oxides were deposited by ultrasonic impregnation on ceramic honeycomb monoliths. Its catalytic performance was evaluated in the combustion of ethanol and n-hexane, VOC molecules of different chemical nature. The catalysts were characterized by N_2 physisorption, SEM-EDS, XRD, X-ray fluorescence, XPS, TPR, TPD-O_2 and OSC measurements. It was observed that the catalyst with the lowest content of Mn-Cu phase was the most active in the combustion of ethanol. This was attributed to the higher content of Mn^{4+} and the increase of lattice oxygen mobility, which would favor a Mars-van Krevelen type mechanism. The catalyst with a medium content of Mn-Cu, proved to be the most active in the combustion of n-hexane. This was associated with a high content of oxygen vacancies and easy availability of oxygen adsorbed on the surface, promoting the combustion of n-hexane, possibly through a Rideal-Eley type mechanism. The catalyst with the highest content of the Mn-Cu phase showed low activity in combustion of ethanol and n-hexane, which was attributed to a higher crystallinity of the Mn-Cu phases generated.

Keywords: Manganese-Copper mixed oxide; Cordierite; Ethanol; n-hexane; VOC oxidation.

1. INTRODUCTION

As a result of the continuous advance in the development of catalytic systems for the organic volatile compounds (VOCs) combustion, the current efforts lead to find new catalysts of transition metals or the optimization of the ones already studied, due to their low cost and especially their high activity and selectivity [1,2]. Although these catalytic systems present some disadvantages, such as those related with the chemical properties, distribution and dispersion of the active phase, which decrease their stability and activity, some systems have shown a similar catalytic performance to those based on noble metals [3]. In this context, it has been demonstrated that the mixture of metal species can induce cooperative effects. This leads to an increase in mobility of oxygens (optimization of the selectivity to the total oxidation), as well as stabilization of the more active catalyst species (activity improvement), so allowing successive reactivation treatments of the catalyst [4].

The Mn-Cu mixed oxides have been successfully employed in catalytic combustion of several VOC molecules and even mixtures of them. They have been used as bulk catalysts as well as supported on monolithic structures by our working group [5-8]. The excellent performance of the Mn-Cu system has been attributed to the formation of low crystallinity oxides and to the presence of $Mn_{1.5}Cu_{1.5}O_4$ incomplete spinel, where manganese in its highest oxidation state (Mn^{4+}) can be found and forms a redox couple with the copper [5].

The catalytic performance of the Mn-Cu system can be optimized by increasing the content of this phase on monolithic supports; but this does not ensure reproduction of the system of phases or the type of interaction that can occur between them. Thus, the complexity of the surface architecture achieved for different catalyst contents can promote different types of adsorption, which also makes possible multiple oxygen supply with different mechanisms involved.

Generally, on metal oxide catalysts, especially in mixed systems, besides the Langmuir-Hinshelwood and Rideal-Eley mechanisms, the Mars-van Krevelen type mechanism (with formation of surface oxygen vacancies as a key step and their subsequent replacement by oxygen of the gas

phase) is dominant [3]. It has been reported that the combustion of oxygenated VOC molecules (alcohols, aldehydes, ketones, etc.) proceeds by a Mars-van Krevelen type mechanism, while combustion of saturated and unsaturated hydrocarbons (n-hexane, propane, toluene, etc.) is carried out by a Riedeal-Eley mechanism or a combination of both mechanisms [9].

In the above context, the aim of this work is to study the effect of increasing the Mn-Cu content over the surface of the monoliths on the type of phases generated. In addition, the relationship between these phases and their catalytic behaviour in the combustion of VOC molecules of different chemical nature has been studied. For this purpose, catalysts with different loading of active phase were tested in the combustion of two representative molecules of each group, an oxygenated molecule as ethanol and a hydrocarbon one as n-hexane.

2. EXPERIMENTAL

2.1. Synthesis of catalysts

Cordierite monoliths were provided by Corning (400 cpsi and 6.5 mil wall thickness) and samples of 10mmx10mmx10mm in laboratory scale were used. The samples were blown with air in order to eliminate particles or dust from the packaging. Then, monoliths were dipped in a colloidal alumina slurry (Nyacol ®), for 10 s and withdrawn to constant speed of 3 cm min^{-1}. The suspension excess was eliminated by blowing air during 45 s. Monoliths were then dried at 120 °C for 1 h. One or two soaks were made and finally the samples were calcined at 500 ºC for 2 h. The monoliths previously coated with alumina were impregnated with aqueous solutions of $(CH_3COO)_2Mn.4H_2O$ and $(CH_3COO)_2Cu.4H_2O$ in a 9:1 molar ratio with a total precursor concentration of 0.4 g ml^{-1}. Monoliths were immersed in the solution and shaken by ultrasound for 1 h. The solution excess was removed by blowing air for 45 s. Finally, they were dried at 80 ºC for 24 h and calcined at 250 ºC for 2 h and 500 °C for 3 h [6,10]. One or two impregnations were made with a calcination treatment in between. The monoliths were called AxCy where A = Alumina, x = 1 or 2 depending on the number

of loads performed, C = Catalyst (Mn-Cu phase), and y = 1 or 2 depending on the number of impregnations performed. The monoliths only coated with alumina were named A1 and A2 corresponding to one or two washcoat loading cycles, respectively. In order to study the reproducibility of the synthesis five specimens were prepared for each catalyst.

2.2 Characterization techniques

The adherence of the coatings was evaluated in terms of the weight loss after exposure of the monoliths to ultrasounds. Monoliths were immersed in 25 ml petroleum ether, inside a sealed beaker, and then treated in an ultrasound bath for 30 min. After that, they were dried at 120 °C for 2 h. The weight loss was gravimetrically determined measuring the weight of the samples both before and after the ultrasonic treatment.

The chemical composition of the catalyst was analyzed by X-ray fluorescence spectroscopy (XRF). A Bruker M4 tornado apparatus, with a voltage of 50 kV, intensity of 200 μA and a multipoint analysis was employed.

SEM images and EDS spectra were obtained using a Quanta 200 scanning electron microscope (Philips) equipped with a Phoenix microanalysis system using a nominal resolution of 3 nm.

The specific surface area of catalysts was calculated by the BET method from the nitrogen physisorption isotherms obtained at -196 °C on samples out gassed at 150 °C using a Micromeritics Accusorb 2100E apparatus.

XRD patterns were obtained by using a Rigaku diffractometer operated at 30 kV and 25 mA by employing V-filtered Cr Kα radiation ($\lambda = 0.2291$ nm).

XPS data were obtained with a Multitecnic UniSpecs equipment with a dual X-ray source of Mg/Al and a hemispheric analyser PHOIBOS 150. Pass energy of 30 eV and an Al anode operated at 100 W was used. The pressure was kept under 29.10^{-8} mbar.

The TPR experiments were performed in a quartz U-type tubular reactor using a TCD as detector. The measurements were made with milled monoliths. Sample amounts were adjusted so as to have 26 mg of Mn-Cu phase in each case. Before each run, the sample was oxidized in a 50 ml min^{-1} flow of 20 vol.%O_2 in He at 300 °C for 30 min. After that, He was admitted to remove oxygen and finally, the system was cooled at 25 °C. The reducing gas was a mixture of 5 vol.% H_2 in N_2, at a total flow rate of 30 ml min^{-1}. The temperature was increased at a rate of 10 °C min^{-1} from room temperature to 700 °C; then it was kept constant at 700 °C until the signal of hydrogen consumption returned to its initial values.

O_2-TPD experiments were performed in a quartz reactor using a TCD as detector. The measurements were made with milled monoliths. Sample amounts were adjusted as above commented, and were pre-treated with helium gas increasing the temperature from room temperature up to 700 °C at 10 °C min^{-1}. The samples were oxidized with a 20% O_2/He mixture at a total flow rate of 30 ml min^{-1} at 700 °C for 30 min. Then, they were cooled down to room temperature in the oxidizing mixture and flushed by a stream of purified He for 30 min. The desorption was carried out in the same conditions as the pre-treatment, maintaining the temperature at 700 °C until the TCD signal returned to baseline.

Oxygen Storage Capacity (OSC) of the catalysts was estimated by means of volumetric oxygen adsorption. Previously the temperature of these experiments was optimized to ensure complete re-oxidation of the catalyst, resulting to be 400 °C. Volumetric adsorption measurements were performed on an automatized analyser, Micromeritics ASAP 2020C. A cleaning treatment with O_2 (5%)/He flow at 500 °C for 1 h, followed by evacuation under high vacuum from 125 °C until room temperature, was performed. Then the sample was reduced in H_2 (5%)/Ar flow at 350 ºC for 1 h, and evacuated at 400 °C for 30 min. Finally, the O_2 adsorption isotherm at 400 °C was recorded.

Loss weight profiles versus time related to the irreversible reduction of the catalysts were recorded using a TA model SDT Q600 thermobalance for samples pretreated in the same way as

those studied by OSC. For the thermogravimetric analysis (TGA), samples were also exposed to a heating program under a flow of H_2 (5%)/Ar (60 ml min^{-1}), with a heating rate of 10 °C min^{-1}.

2.3. Catalytic tests

The monolithic catalysts were evaluated in the combustion of ethanol and n-hexane. The reacting stream was 500 cm^3 min^{-1} with a composition of C2H5OH:O_2:N_2 = 0.25:20.94:78.81 for ethanol and C6H14:O_2:N_2 = 0.14:20.97:78:89 for n-hexane. Before to the catalytic tests, the samples were subjected to pretreatment at 350 ° C in reaction flow for 8 h. The gaseous mixtures were analyzed by gas chromatography using a Buck Scientific Mod 910 with a FID detector, a methanizer and a Carbowax 20M/Chromosorb W column. The conversion of VOC, X%, is defined as the percentage of VOC feed that is reacted. Intrinsic activity (moles converter VOC $g^{-1}h^{-1}$) was calculated by the following expression:

$$\frac{mol}{g.h} = \frac{X_{COVs}.F}{m_{cat.} \times 100}$$

where X_{VOCs} is the conversion rate at a given temperature (%), F is the flow of VOCs (mol_{voc} h^{-1}) and $m_{cat.}$ the mass of catalyst or active phase deposited (g).

The stability test was carried out under extreme reaction conditions. The catalysts were evaluated in the combustion of n-hexane, with the same composition of the feed stream, for 40 h at a temperature higher than the total combustion temperature, 350°C. Conversion measurements were taken every 25°C until reaching 100% conversion. When this conversion level was reached, the temperature was increased to 350°C and held for 12 h. Then the temperature was decreased to room temperature and again the light-off curve was lifted. This was repeated once again, obtaining 3 complete light-off curves. T_{50} values (50% conversion temperatures) and T_{90} (90% conversion temperature) were obtained from the light-off curves at different times, i.e., 8 h, 20 h and 40 h (Figure 10).

3. RESULTS AND DISCUSSION

3.1. Synthesis of the catalysts

Both, the alumina deposition method (washcoating), and the one employed to deposit the Mn-Cu (ultrasonic impregnation) leaded to a quite reproducible final composition of the catalysts. Data corresponding to the whole set of preparations performed for each catalyst are shown in Table S1 of Supporting Information, and demonstrate the above. Meanwhile, the Table 1 summarizes the average data of both Al_2O_3 and Mn-Cu phase incorporated to the monolith substrate. Monoliths with one charge of alumina had an average of 7.2% mass gain, while for those with two loads; the average percentage of gain was 12.7%. Regarding the catalytic phase, for the same Al_2O_3 load (A1C1 and A1C2), an increase in mass of the Mn-Cu phase of about 28% is observed; while for two loads of catalytic phase, the mass gain is about 45% with increasing the load of alumina (A1C2 and A2C2).

The two phases deposited over the cordierite monoliths (Al_2O_3 and Mn-Cu), with different loads, presented an excellent stability, since the load loss percentages obtained with the adherence test are very small (< 1.12 %) for the three catalysts (Table 1).

Taking into account the influence of the Mn/Cu ratio on the generated catalytic phases, its quantitative estimate should be addressed. As can be seen in Table 1, the experimentally obtained Mn/Cu molar ratios for the three catalysts were lower than the Mn/ Cu = 9/1 molar ratio of the precursor impregnating solution. The lower values of Mn/Cu molar ratio could be associated with a selective adsorption of copper in relation to manganese species during the ultrasonic impregnation.

Comparison between the SEM images of bare cordierite and the A2C2 catalyst (Figure S1) allows evidencing certain differences. In particular, the roughness originally present on the surface of the ceramic support seems to decrease on the catalysts. This should be related to the deposition of both the alumina and Mn-Cu phase. In this sense, acquisition of EDS compositional data permitted identifying the active phase. Similar results were obtained for A1C1 and A1C2 samples.

As well known, deposition of alumina onto cordierite monoliths, before incorporating the catalyst, is usually aimed at increasing the surface area and favouring the catalyst anchoring. As can be seen in Table 1, the surface area of the ceramic monoliths increased from less than 1 m^2 g^{-1} to 9 m^2 g^{-1}. The deposition of a second alumina load further increased the S_{BET} area by about 40%. It was also observed that for the same alumina load, the increase in the number of Mn-Cu loads did not significantly change the S_{BET} area. However, the increase in the number of alumina loads, for the same number of Mn-Cu loads, increased the specific surface area. This increase is the same as that observed in the S_{BET} values of cordierite with 1 and 2 alumina loads. Therefore, it is the amount of alumina phase the main responsible for the changes in the BET specific surface area.

The inset of Figure 1 shows the physisorption isotherms obtained for all monoliths. All the samples exhibited type IV isotherms with H1 hysteresis cycle, according to the IUPAC classification, corresponding to mesoporous solids [11]. The pore size distribution (Figure 1) for A1 showed a wide range of distribution with a maximum around 93 Å accompanied by a shoulder at 43 Å. When a second load of alumina was applied the distribution, range was significantly narrowed and the maximum diminished down to about 70 Å, with the shoulder slightly displaced to approx. 40 Å. These observations are in good agreement with the changes in the BET parameter above discussed. The incorporation of the catalytic phase onto the A1 sample also modifies the pore structure (see A1C1 and A1C2 curves). The change observed suggests that the Mn-Cu phase is being deposited over a non-homogeneous support consisting on the cordierite partially covered by the alumina. This effect does not occur when the catalytic phase is deposited over the A2 support. Notice how the A2C2 curve resembles that of A2. In this case, the Mn-Cu phase can be considered to reproduce the surface of the alumina with a minimum catalyst layer thickness. Also remarkable, the changes in the relative intensity of the peak corresponding to mesopores with size around 70 Å reflect the relative variation of the S_{BET} in Table 1.

3.2. Structural characterization

Figure 2 shows the XRD diffractograms corresponding to bare cordierite used as support, reference alumina (Nyacol) and the A2C2 catalyst as representative of the Mn-Cu-containing samples. This study did not provide any information about the phases generated in the Mn-Cu supported catalysts due to the high intensity of the cordierite diffraction lines (PDF 01-084-1220), which is the majority phase. In addition, reflections attributable to δ-Al_2O_3 (PDF 00-016-0394) and α-$Al(OH)_3$ (PDF 00-012-0460) were hardly identified, these corresponding to the calcined suspension of Nyacol.

Considering the surface nature of the generated catalytic phases and their relative low concentration XPS technique was required. For all spectra the load effect was corrected by adjusting the binding energy of C1s to 284.6 eV [12].

For the three catalysts, the position of the signals Cu2p3/2 and Cu2p1/2 corresponds to Cu^{2+} (934.5 eV and 954.2 eV, respectively), which is also confirmed by the presence of the "shake up" located between these two signals [13-15] (Figure 3). The signals located in the regions between 640.0-650.0 eV and 650.0-660.0 eV correspond to Mn2p3/2 and Mn2p1/2, respectively for all catalysts (Figure 4.a) [16,17].

O1s spectra are shown in Figure 4.b. According to the signal position, three types of oxygen species can be identified: signals at low bond energies (O_L: 529.8-530.1 eV) can be associated with the lattice oxygens (O_2^{2-}); intermediate bond energy signals (531.3 eV) are related to surface adsorbed oxygen species (O_2^- or O^-), OH^- groups and oxygen vacancies; and finally signals at high bond energies (533.0 eV) can be associated with adsorbed water molecules [12,18,19]. Signals corresponding to O1s were deconvoluted only in two components (Figure 4.b). In Table 2 it can be observed that for the three catalysts the content of surface oxygen species and/or oxygen vacancies, considered the most active oxygen [20-22], is the majority, exceeding 50%. A1C2 presents the highest percentage (57%) for this type of oxygen species, and also a shift of its signal to lower

binding energy. Xingyi et al. [23] observed this behavior in MnO_x-CeO_2 catalysts. They observed that when the Mn/(Mn+Ce) ratio increased, the signal energy of active oxygen (O_A) decreased. This behaviour was related to an electron transfer process "Mn← O", which allows the formation of very active electrophilic oxygen species (eg. O_2^-, O^-, O^-), which are oxygen species active mainly in mechanisms of superficial reactions (Rideal-Eley mechanism). As can be seen in Table 2 for the (Mn/Mn+Cu) ratio, the catalyst A1C2 shows this behavior, which could justify the higher percentage of O_A.

For all catalysts, the Mn/Cu surface atomic ratio is lower than the theoretical ratio; its values being very similar to those measured by X-ray fluorescence. Taking into account that one is a bulk technique (XRF) and the other is a surface technique (XPS), these results would indicate that the phase arrangement achieved at the surface of the catalyst is replicated in the bulk thereof. This characteristic can be associated to a minimum catalyst layer thickness, as observed from the textural study performed by means of N_2 physisorption.

The A1C2 catalyst has the highest surface manganese content, relative to the rest of the catalysts. From the (Mn + Cu)/Al ratio the dispersion degree of the Mn-Cu phase on the alumina could be estimated. A1C2 showed the highest dispersion, while A1C1 showed the lowest one (Table 2).

One of the major problems in the chemistry of non-stoichiometric transition metal oxides is the determination of the oxidation states and their relative amounts. This is particularly problematic for manganese oxides, owing to their multiple oxidation states and overlapping binding energies for them. It has been reported that the relative abundance of Mn^{2+} (640.9 eV), Mn^{3+} (641.9 eV) and Mn^{4+} (643.3 eV) species can be obtained by Mn2p3/2 deconvolution (Table 3) [12,22.23].

The spectrum shown in Figure 4.a was deconvoluted in two components corresponding to Mn^{3+} (641.9 eV) and Mn^{4+} (643.3 eV) for all catalysts. As shown in Table 3, A1C1 is the catalyst with the highest Mn^{4+} content, while A1C2 has the highest percentage for the Mn^{3+} oxidation state. A2C2 catalyst presents a higher percentage for Mn^{4+} and a lower Mn^{3+} one than A1C2 catalyst. However,

there is a controversy about the certainty of the XPS deconvolution results of the Mn spectra. Therefore it is necessary to discuss these results in conjunction with the rest of the characterization techniques.

3.3. Chemical characterization

In Figure 5 the signals corresponding to the reduction with H_2 of the three catalysts are presented. It can be seen that the reduction $T_{on\ set}$ (temperature at which the reduction reaction begins) increased with increasing the Mn-Cu phase and the alumina loadings, being A2C2 the catalyst that presented the higher $T_{on\ set}$ (Table 4). The TPR technique allows obtaining information about the arrangement and interaction that can occur between the generated phases and even a reducibility-activity relationship can be established. It has been reported that in the oxidation of hydrocarbons that occurs by a Mars-Van Krevelen type redox mechanism the more easily the catalyst can be reduced the higher activity exhibits [24,25]. In our case, the catalyst with the greatest reducibility is A1C1 (greater reducibility corresponds to a lower reduction start temperature, $T_{on\ set}$), whereas A2C2 is the least reducible. These results show linearity with the catalytic behavior (intrinsic activity) in the combustion of ethanol, as it will be shown later.

For the A1C1 catalyst two intense reduction signals (264 and 290 ºC) and two shoulders (231 and 320 ºC) were observed. In the case of A1C2 the relative intensities of the two most intense peaks reversed and the first one moved to higher temperatures (268 °C). A2C2 presented three overlapping reduction signals at 286, 310 and 339 °C, the first one being the most intense. For the three catalysts, the signal located at 264 °C, 268 °C and 286 °C has been attributed to the Cu reduction, and the rest of the signals to the Mn reduction in different oxidation states and/or different arrangement [6,10].

It has been reported for mixed Mn-Cu systems that the reduction signals at low temperatures can be associated to the reduction of Mn^{4+} ions present in the mixed phase $Mn_{1.5}Cu_{1.5}O_4$ or to the existence of structural defects associated to surface oxygen vacancies and/or the high dispersion of Mn_2O_3 [5,6]. In the A1C1 reduction curve, the shoulder with its maximum at 231 °C can be directly related

to this type of signals. In Figure 5 it can be seen that the area of the reduction signals below 237 °C (selected temperature to approximately take the end of reduction of the Mn^{4+} species as a reference), decreases with the increase in the Mn-Cu phase content. If the areas are expressed as the H_2 consumption per gram of Mn-Cu phase, it can be seen in Table 4 that the A1C1 catalyst has a H_2 consumption that is approximately four times that shown by the rest of the catalysts, which is consistent with data obtained by XPS, as this technique indicated that A1C1 sample is the one having highest Mn^{4+} content. The combination of both results also suggest that the external surface composition resembles that of the bulk. The consumption of H_2 up to 350 °C (temperature that ensures 100% conversion of any of the tested VOCs) shows an order equal to: A1C1 > A2C2 > A1C2.

Taking into account that the TPR investigation only provides information about the reduction of the samples under dynamic conditions with increasing temperatures, it was decided to perform also ultimate OSC experiments, which would give a good approximation for the thermodynamic limit of the oxygen release process for samples previously reduced at 350 °C and evacuated at 400 °C. Figure 6 shows the O_2 volumetric isotherm at 400 °C for the A2C2 monolith previously reduced at 350 °C, as representative of the investigated catalysts. The shape of the isotherm suggests that O_2 chemisorption occurs very rapidly so that complete re-oxidation of the catalysts already occurs at very low oxygen pressures. OSC values of the three catalysts derived from the isotherms are shown in Table 4. As can be seen, A1C2 presented the highest oxygen storage capacity, followed by the A1C1, and the A2C2 presented the lowest capacity. It should be emphasized that a high oxygen storage capacity does not necessarily imply a fast release of the oxygen. In this sense, complementary information was obtained through thermogravimetric experiments in which the loss weight profiles versus time related to the irreversible reduction of the catalysts was monitored for the isothermal step (1 h) corresponding to the treatment under H_2/Ar flow at 350 ºC (Figure 7). The TGA curves obtained give indications concerning the kinetics of the reduction process. Notice how in

A1C1 and A1C2 90% of the total oxygen release occurs within the first 10 minutes of the isothermal treatment, while for A2C2 more than 30 minutes are necessary.

The mechanism by which the combustion of a given VOC proceeds not only depends on the maximum amount of oxygen available and the easiness to mobilize this but it has been also related to the types of oxygen present in the catalyst [26]. For this purpose, an O_2-TPD investigation was also performed. In general, two signals of desorption are observed: α- and β-oxygen, which correspond to surface oxygen and oxygen of the crystalline lattice, respectively. The α-oxygens are adsorbed on the surface vacancies and are released at low temperature (< 400 °C). β-oxygens are observed at higher temperatures (> 400 °C) and come from the bulk of the catalyst. Therefore, α-oxygen participates in the surface reaction mechanism (Rideal-Eley mechanism), while β-oxygen is important when high oxygen mobility in the catalyst is required to complete the redox cycle (as is the case of the Mars-van Krevelen mechanism).

In our case (Figure 8) the α-oxygen type must be related to broad asymmetric peak ranging approximately from 100 °C to 400 °C, demonstrating the diversity of phases generated. The relative maximum for all the catalysts is located between 120 and 180 ºC. In the particular case of A1C1 shoulders around 326 °C and 394 °C can be also resolved. The intensity of the α-oxygen signal follows the order A1C1 ≈ A1C2 > A2C2. Nevertheless, A1C1 and A1C2 show significant differences in the temperature at which the oxygen release starts, being 60 ºC higher in the former. This would mean a higher availability of the surface vacancies adsorbed oxygen in the A1C2 catalyst. Regarding the β-oxygen species, it should be noticed that in the case of A1C1 sample its corresponding peak maximum is advanced 50 ºC respect to A1C2, this indicating a higher availability of the lattice oxygen in the former. Finally, for the A2C2 sample the ratio between the intensities related to α and β species is clearly lower in good agreement with XPS O_A/O_L values (Table 2). In several works in which the catalytic activity of different manganese oxide phases in oxidation reactions is studied [27,28] phases with lower crystallinity according to XRD are related

with a higher relative content of α oxygen species as detected by O_2-TPD. This allows concluding that the A2C2 catalyst must be the sample with the highest crystallinity degree.

3.4. Catalytic test

Ethanol and n-hexane are VOCs representative molecules presented in several industrial effluents. Both molecules have different chemical nature, ethanol represents the group of oxygenated VOCs, while n-hexane belongs to the hydrocarbon group of linear chain. Our catalysts were evaluated in the combustion of both molecules, at four different temperatures (Figure 9). The carbon balance was closed at ±5% for both reactions. In the ethanol combustion, at 100% of conversion, CO_2 and H_2O were obtained as products of total combustion, and at lower temperatures or lower conversion levels, acetaldehyde was detected as product of incomplete combustion.

The A1C1 and A1C2 catalysts showed approximately the same catalytic behaviour while A2C2 showed lower activity for the four tested temperatures. At 200 °C this catalyst was approximately 20% less active than A1C1 and A1C2. In general, the catalytic activity is considered a function of the active phase content, the greater the mass of catalyst, the more active sites are available, and consequently, a greater activity. However, the studied Mn-Cu catalysts do no present the same performance for catalytic evaluation of ethanol, since it would be expected an order of activity as A2C2 > A1C2 > A1C1. It is evident that for a catalytic system constituted by Mn and Cu oxides, there is an arrangement of the phases that depends on the Mn-Cu-O mass that is not subject to the influence of the support surface (alumina). All Mn oxides could provide catalytic sites capable of activating VOCs, but their "quality" would not be the same.

In order to evaluate the efficiency of the catalytic sites generated in each catalyst, we calculated the intrinsic activity (defined as moles of VOC consumed per gram of active phase per hour) to avoid the effect of the active phase content. As shown in Figure 9, in this case the order obtained was A1C1 > A1C2 > A2C2. The more efficient ethanol combustion shown by the active sites of the

A1C1 catalyst, in comparison with the other two catalysts, is demonstrated by the large difference in the numbers of moles converted at the same temperature, and throughout the temperature range in which was evaluated.

The catalysts were also evaluated in the combustion of n-hexane under the same conditions as for ethanol. During the catalytic evaluation of this VOC only CO_2 and H_2O were obtained as reaction products at all temperatures tested. Total conversion of n-hexane was achieved at 345 °C (A1C1), 327 °C (A1C2) and 340 °C (A2C2). As shown in Figure 9, the order of activity is different to the activity performed with the ethanol, being: A2C2 ≈ A1C2 > A1C1. In this case, it could be considered a small effect of the active phase content on the catalytic behaviour. However, in terms of intrinsic activity, active sites of the A1C2 catalyst were more efficient, followed by sites of the A1C1 catalyst and the less efficient sites for the combustion of n-hexane as ethanol were those of the A2C2 catalyst. The results of intrinsic activity of the three catalysts, in the combustion of ethanol and n-hexane, showed that according to the chemical nature of the VOC molecule, the type of phases generated in A1C1 and A1C2 monoliths provide a different activity for each VOC, while for A2C2 the behaviour is the same for both molecules.

It is generally accepted that the oxidation of VOCs on noble metals involves the dissociative adsorption of oxygen, followed by the Langmuir-Hinshelwood mechanism (reaction with chemisorbed reagent) or the Rideal-Eley mechanism (reaction with reagent in the gas phase), depending on the nucleophilic character of the organic reagent [3]. On metal oxide catalysts, especially mixed systems, catalytic combustion of VOC molecules of different chemical nature can be carried out by different mechanisms. In general, Rideal-Eley mechanism for hydrocarbons and Mars-van Krevelen mechanism (with formation of surface oxygen vacancies as key step and its subsequent replacement by oxygen from the gas phase) or a combination of both mechanisms for oxygenate compounds [3]. The efficiency of the catalysts in carrying out each mechanism depends directly on their ability to mobilize the different oxygen species involved in them.

From the results obtained by the structural and chemical characterization of the catalysts, their catalytic performance could be interpreted as follows:

1) The low catalytic activity of the A2C2 catalyst in the combustion of both molecules can be directly associated to the formation of higher crystallinity phases (O_2-TPD and XPS results), where the content (low OSC data) and mobility (high $T_{on\ set}$ in TPR experiments and slow oxygen release in TGA measurements) of both the oxygen adsorbed in vacancies and lattice oxygen are smaller. Thus, whatever the mechanism by which the oxidation of the VOC molecule is carried out, its catalytic performance must be low.

2) The amount and nature of the deposited Mn-Cu phase has a significant effect on the catalytic behaviour. The type of phases generated by the deposition of Mn-Cu as a function of reached loading determine the mechanism of the oxygen supply for the combustion of VOC. This also affects the activity in different way depending on the chemical nature of the VOC molecule to be burned.

3) The A1C2 catalyst proves to be more efficient in the combustion of n-hexane. This could be explained by considering the possibility that the n-hexane combustion is carried out by the Rideal-Eley type mechanism. This mechanism involves the dissociative adsorption of oxygen in surface vacancies. According to the OSC study this sample has the highest content of oxygen vacancies. Moreover, the O_2-TPD profile indicated a more mobile oxygen considering its desorption at lower temperature.

4) A1C1 is more active in the combustion of ethanol, which we suggest that is carried out mainly by the Mars-van Krevelen type mechanism. This mechanism requires the ability to mobilize oxygen from the lattice of the catalytic phases. Although this catalyst has a lower oxygen storage capacity than A1C2, it seems to have greater ability to mobilize the lattice oxygen, as denoted by the high temperature region of the O_2-TPD profile.

The stability of the catalysts under reaction conditions is one of the main characteristics of a good catalyst. Therefore, the three catalysts were subjected to extreme reaction conditions. The catalysts

were evaluated for 40 h at a temperature higher than the total combustion temperature (350 ° C). The stability tests were made with n-hexane, the molecule which is the most difficult to oxide compared with ethanol. As can be seen in Figure 10, the three catalysts showed excellent catalytic stability over time. The temperatures of 50% (T_{50}) and 90% (T_{90}) conversion of n-hexane show no appreciable variations during the 40h evaluation. The concentration of the reaction products under the conditions of evaluation of the stability test is the highest. Therefore, it may also be considered that the reaction products do not affect the catalytic performance of the catalysts.

4. CONCLUSIONS

Ceramic monoliths with different alumina and Mn-Cu mixed oxide loads were successfully synthesized by ultrasonic impregnation. The alumina (washcoating) and active phase deposition techniques showed high reproducibility, obtaining stable thin deposited layers.

All the monoliths showed very good activity and stability in the combustion of ethanol and n-hexane. It was observed that the active phase content, its consequent structural and chemical nature, influences the type of mechanism by which the VOC combustion is carried out.

Control of the deposited catalyst load is decisive for favouring the type of operating VOC combustion mechanism. A minimum of Mn-Cu oxide load leads to the formation of phases that would favour the combustion to proceed through a redox mechanism, such as Mars-van Krevelen. This behaviour could be associated with the higher content of Mn^{4+} (higher reducibility) and its greater facility in the mobilization of lattice oxygen. As a consequence, the samples with these properties show better performance in the combustion of ethanol.

In samples with high content of oxygen vacancies and good mobility of the oxygen adsorbed on them, is considered combustion proceeds through a Rideal-Eley type mechanism. As a result, these catalysts are better for combustion of n-hexane.

Finally, a higher Mn-Cu content in the preparation of the catalyst favours a higher degree of crystallinity in the deposited phase. In this case, the samples are characterized by a lower catalytic activity in the combustion of both VOC molecules.

This research is of interest in the context of the most suitable design of catalysts consisting of mixed oxides deposited onto structured supports for the combustion of VOCs as a function of their nature, either saturated and unsaturated hydrocarbons or alcohols.

5. ACKNOWLEDGMENT

The authors would like to thank the Universidad Nacional de San Luis (UNSL), Agencia Nacional de Promoción Científica y Tecnológica (ANPCyT) and Consejo Nacional de Investigaciones Científicas y Técnicas (CONICET). Also, we are grateful to the Spanish Project MINECO/FEDER/Ref: MAT2013-40823-R and the Junta Andalucía (FQM-110 group). The XPS measures are appreciated to INCAPE-CONICET. They also acknowledge the SC-ICYT of Cadiz University for using its XRD and electron microscopy division facilities.

6. REFERENCES

[1] Aguilera DA, Perez A, Molina R, S. Moreno. Cu-Mn and Co-Mn catalysts synthesized from hydrotalcites and their use in the oxidation of VOCs. Appl Catal B: Environmental 2011;104:144-150.

[2] Li WB, Wang JX, Gong H. Catalytic combustion of VOCs on non-noble metal catalysts. Catal. Today 2009;148:81-87.

[3] Spivey JJ. Complete catalytic oxidation of volatile organics. Ind. Eng. Chem. Res. 1987;26:2165-2180.

[4] Garetto T, Loguburu I, Montes M. Eliminación de emisiones atmosféricas de COVs por catálisis y adsorción, CYTED, Madrid, 2008.

[5] Morales MR, Barbero BP, Cadus LE. Total oxidation of ethanol and propane over Mn-Cu mixed oxide catalysts. Appl. Catal. B: Environmental 2006;67:229-236.

[6] Morales MR, Barbero BP, Cadus LE. Evaluation and characterization of Mn-Cu mixed oxide catalyst for ethanol total oxidation: Influence of copper content. Fuel 2008;87:1177-1186.

[7] Morales MR, Barbero BP, Cadus LE. MnCu catalyst deposited on metallic monoliths for total oxidation of volatile organic compounds. Catal. Lett. 2011;141:1598-1607.

[8] Aguero FN, Morales MR, Barbero BP, Cadus LE. MnCu supported on ceramic monoliths for catalytic combustion of Volatile Organic Compounds. Chem. Eng. Technol. 2013;36:1-7.

[9] Aguero FN, Barbero BP, Gambaro L, Cadus LE. Catalytic combustion of volatile organic compounds in binary mixture over $MnOx/Al_2O_3$ catalyst. Appl. Catal. B: Environmental 2009;91(1-2):108-112.

[10] Ferradon M, Carno J, Jaras S, Bjornbon E. Total oxidation catalysts based on manganese or copper oxides and platinum or palladium I: Characterisation. Appl Catal A 1999;180:141–51.

[11] Neimark AV, Sing KSW, Thommes M. Characterization of Solid Catalysts. In: Eartl G, Knözinger H, Weitkamp J, editors. Handbook of Heterogeneous Catalysis, vol. 3, 2nd Ed. Wiley-CCH, Weinheim, Alemania, 2008, p. 721-738.

[12] Santos VP, Pereira MFR, Orfao JJM, Figueiredo JL. The role of lattice oxygen on the activity of manganese oxides towards the oxidation of volatile organic compounds. Appl. Catal. B 2010;99:353-363.

[13] Avgouropoulos G, Ioannidesa T, Matralis H. Influence of the preparation method on the performance of $CuO-CeO_2$ catalysts for the selective oxidation of CO. Appl. Catal. B 2005;56:87-93.

[14] Zhu P, Li J, Zhou S, Zhou R. Preferential oxidation properties of CO in excess hydrogen over $CuO\text{-}CeO_2$ catalyst prepared by hydrothermal method. Appl. Surf. Sci. 2008;255:2903-2909.

[15] Cocke DL, Veprek S. First direct evidence of a solid state charge transfer redox system $Cu^{+2} + Mn^{3+} \leftrightharpoons Cu^{1+} + Mn^{4+}$in copper manganese oxide, Sol. State Comm. 1986;57:745-748.

[16] Iwanowski RJ, Heinonen MH, Paszkowicz W, Minikaev R, Story T, Witkowska B. X-ray photoelectron study of $Sn_{1-x}Mn_xTe$ semimagnetic semiconductors, Appl. Surf. Sci. 2006;252:3632-4364.

[17] Nesbitt HW, Benerjee D. Interpretation of XPS Mn(2p) spectra of Mn oxyhydroxides and constraints on the mechanism of MnO_2 precipitation, Am. Mineral. 1998;83:305-315.

[18] Jiratova K, mikulova J, Klempa J, Grygar T, Bastl Z, Kovanda F. Modification of Co-Mn-Al oxide with potassium and its effect on deep oxidation of VOC, Appl. Catal A 2009;362:106.

[19] Kang M, Park ED, Kim JM, Yie JE. Appl. Catal. A 2007;327:261-269.

[20] Harris KDM, Edwards PP. Turning Points in Solid. State Materials and Surface Science, RCS Publishing, Cambridge, 2008, 568-576.

[21] Zawadzki M, Trawczynski J. Synthesis, characterization and catalytic performance of LSCF perovskite for VOC combustion, Catal. Today 2011;176:449-452.

[22] Piumetti M, Fino D, Russo N. Mesoporous manganese oxides prepared by solution combustion synthesis as catalysts for the total oxidation of VOCs, Appl. Catal. A 2015;163:277-287

[23] Xingyi W, Qian K, Dao L. Catalytic combustion of chlorobenzene over $MnOx–CeO_2$ mixed oxide catalysts, Appl. Catal. B 2009;86:166-175.

[24] Reddy BM. Redox Properties of Metal Oxides. In: J.L.G. Fierro, editor. Metal Oxides: Chemistry and Applications. CRC Press Taylor & Francis, Florida, USA, 2005, p. 215-246.

[25] Dula R, Janik R, Machej T, Stoch J, Grabowski R, Serwicka EM. Mn-containing catalytic materials for the total combustion of toluene: The role of Mn localization in the structure of LDH precursor, Catal. Today 2007;119:327-331.

[26] Seiyama T, Yamazoe N, Eguchi K. Characterization and activity of some mixed metal oxide catalysts, Ind. Eng. Chem. Prod. Res. Dev. 1985;24:19-27.

[27] Jia J, Zhang P, Chen L. The effect of mophology of α-MnO_2 on catalytic decomposition of gaseous ozone, Catal. Sci. Technol. 2016;6:5841-5847.

[28] Genuino HC, Dharmarathna S, Njagi EC, Mei MC, Suib SL. Gas-phase total oxidation of benzene, toluene, ethylbenzene, and xylenes using shape-selective manganese oxide and copper manganese oxide catalysts, J. Phys. Chem. C 2012;116:12066-12078.

TABLES

Table 1. Main characteristics of the samples studied, including adherence, textural and compositional data.

Sample	Al_2O_3 retained load (%)	Mn-Cu retained load (%)	Weight loss (%)[a]	S_{BET} (m^2/g)	Mn/Cu molar ratio[b]
A1C1	7.06 ± 0.4	3.48 ± 0.1	0.56	9.5	6.6
A1C2	7.08 ± 0.3	4.53 ± 0.1	0.89	10.5	6.5
A2C2	12.72 ± 1.0	7.49 ± 0.3	1.12	17.3	5.4
Cordierite	n.a.	n.a.	n.a.	0.4	n.a.
A1	7.0	n.a.	1.25	9.0	n.a.
A2	12.5	n.a.	0.20	14.5	n.a.

[a] Weight loss (%) estimated from adherence test, considering both active phase and alumina loads.

[b] Obtained by means of X-ray fluorescence (XRF).

[n.a.] Not applicable

Table 2. Binding energies and surface atomic ratios from XPS.

Catalysts	O 1s					Mn/Cu	Mn/(Mn+Cu)	Mn+Cu/Al
	O_A		O_L		O_A / O_L			
	BE (eV)	atom. %	BE (eV)	atom. %				
A1C1	532.4	55.2	530.8	41.5	1.4	6.2	0.86	0.12
A1C2	532.2	57.4	530.6	39.2	1.5	7.0	0.88	0.32
A2C2	532.4	52.6	530.8	44.4	1.2	5.3	0.84	0.21

O_A and O_L correspond to surface adsorbed and lattice oxygen, respectively

Table 3. Results of curve-fitting on the $Mn2p_{3/2}$ peaks in XPS spectra of the three catalysts: the atomic percentage for Mn^{4+} and Mn^{3+} is reported.

Catalysts	Mn^{4+} (atom.%)	Mn^{3+} (atom.%)
A1C1	63	37
A1C2	48	52
A2C2	54	46

Table 4. Redox properties of the catalysts, including quantitative data corresponding to the TPR study and OSC measurements.

Catalysts	$T_{on\ set}$ (°C)[a]	H_2 consumption up to 237 °C (µmol H_2 g^{-1})	H_2 consumption up to 350 °C (µmol H_2 g^{-1})	OSC (mmol O_2/g Mn-Cu)[b]
A1C1	86	402	1640	3.1
A1C2	129	103	1140	3.9
A2C2	143	96	1300	2.2

[a] Temperature at which the reduction process begins.

[b] Estimated by means of oxygen volumetric adsorption on catalysts reduced at 350 ºC.

FIGURES CAPTIONS

Figure 1. Pore size distribution and N_2 physisorption isotherms of the samples investigated.

Figure 2. XRD diffractograms of bare cordierite (a), calcined Al_2O_3 (Nyacol) (b) and A2C2 (c) samples. The alumina sample was obtained by drying the suspension at 120 °C for 48 h and further calcination for 2 h at 500 °C.

Figure 3. Cu2p XPS spectra of the catalysts.

Figure 4. a) Mn $2p_{3/2}$ and b) O 1s XPS spectra of the catalysts.

Figure 5. TPR study of the catalysts. On set temperature for the reduction process and temperature range selected for the quantitative analysis of the traces are shown.

Figure 6. O_2 volumetric isotherm at 400 °C of the A2C2 catalyst previously reduced at 350 °C and evacuated at 400 ºC.

Figure 7. Normalized weight loss obtained by thermogravimetry corresponding to the treatment (1 h) under H_2(5%)/Ar flow at 350 ºC prior to the OSC measurement.

Figure 8. O_2-TPD diagrams of the catalysts.

Figure 9. Conversion and intrinsic activity obtained for the VOCs combustion.

Figure 10. Stability tests on the combustion of n-hexane. Temperatures corresponding to 50% (T_{50}) and 90% (T_{90}) conversion as a function of reaction time.

Figure 1

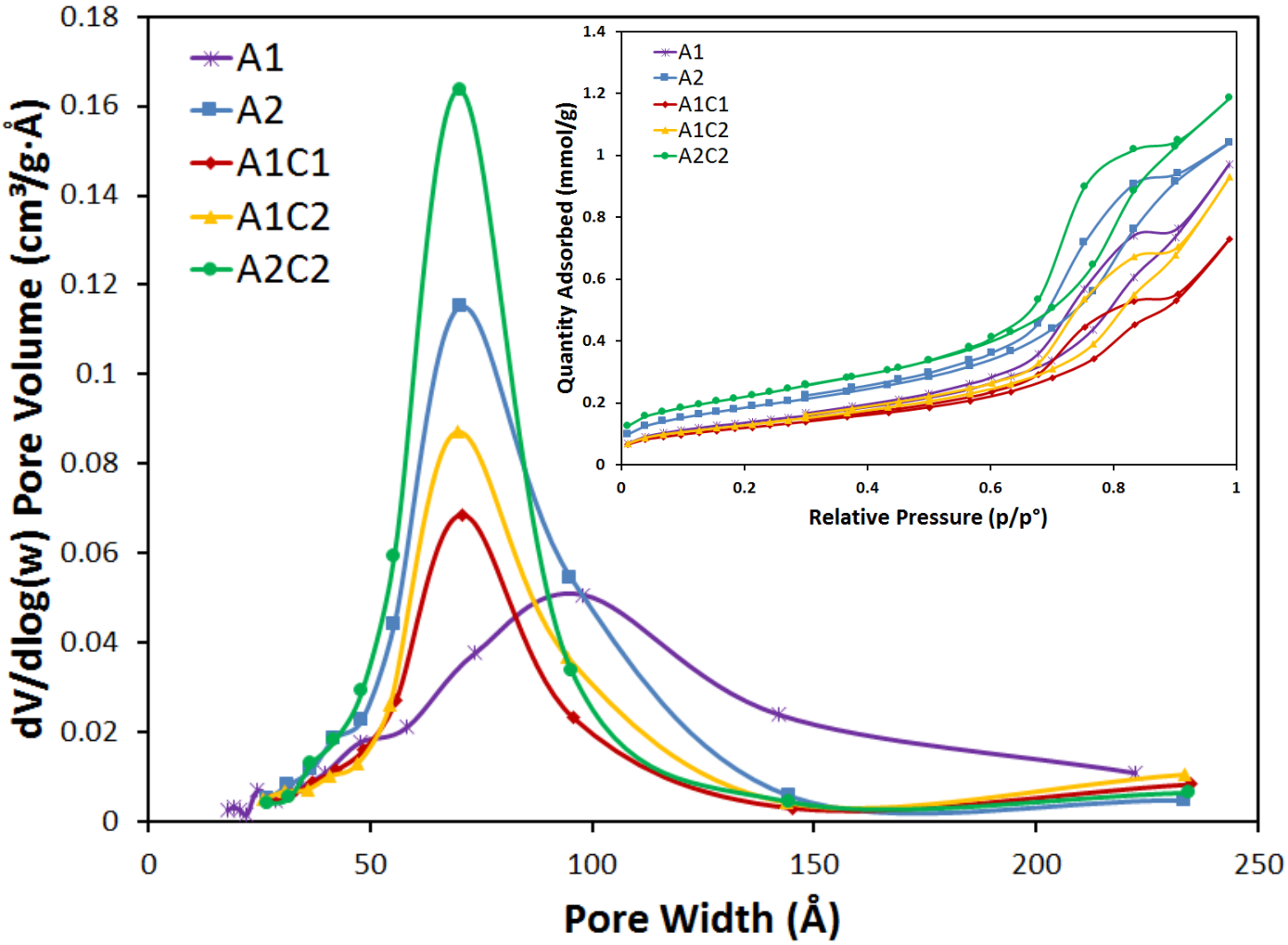

A1
A2
A1C1
A1C2
A2C2
dV/dlog(w) Pore Volume (cm³/g·Å)
Pore Width (Å)
0.18
0.16
0.14
0.12
0.1
0.08
0.06
0.04
0.02
0
0
50
100
150
200
250
Quantity Adsorbed (mmol/g)
Relative Pressure (p/p°)
1.4
1.2
1
0.8
0.6
0.4
0.2
0
0.2
0.4
0.6
0.8
1

Figure 2

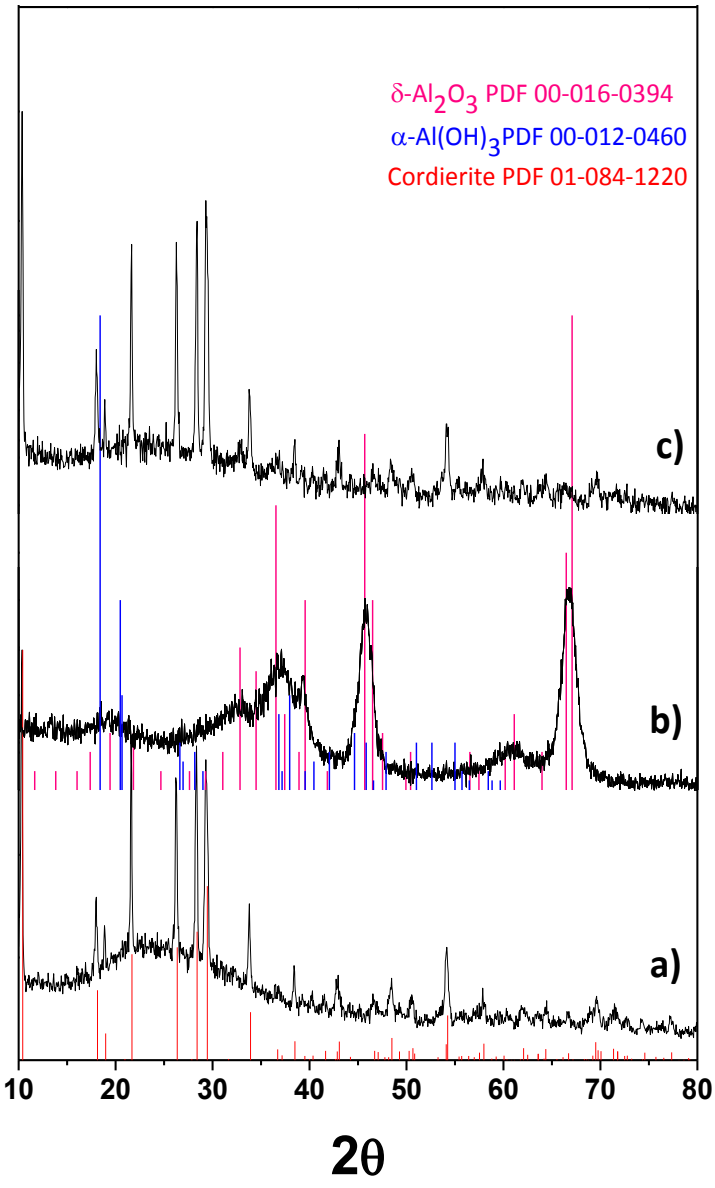

δ-Al2O3 PDF 00-016-0394
α-Al(OH)3PDF 00-012-0460
Cordierite PDF 01-084-1220
c)
b)
a)
10
20
30
40
50
60
70
80
2θ

Figure 3

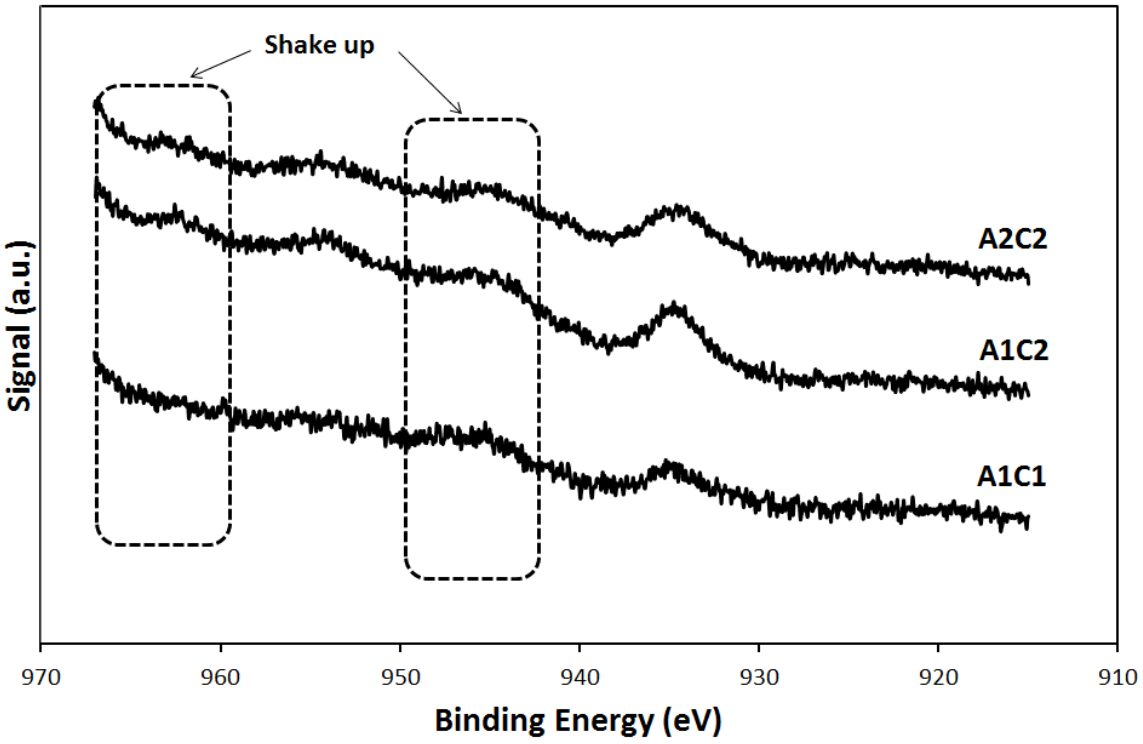

Shake up
A2C2
A1C2
A1C1
Signal (a.u.)
970
960
950
940
930
920
910
Binding Energy (eV)

Figure 4

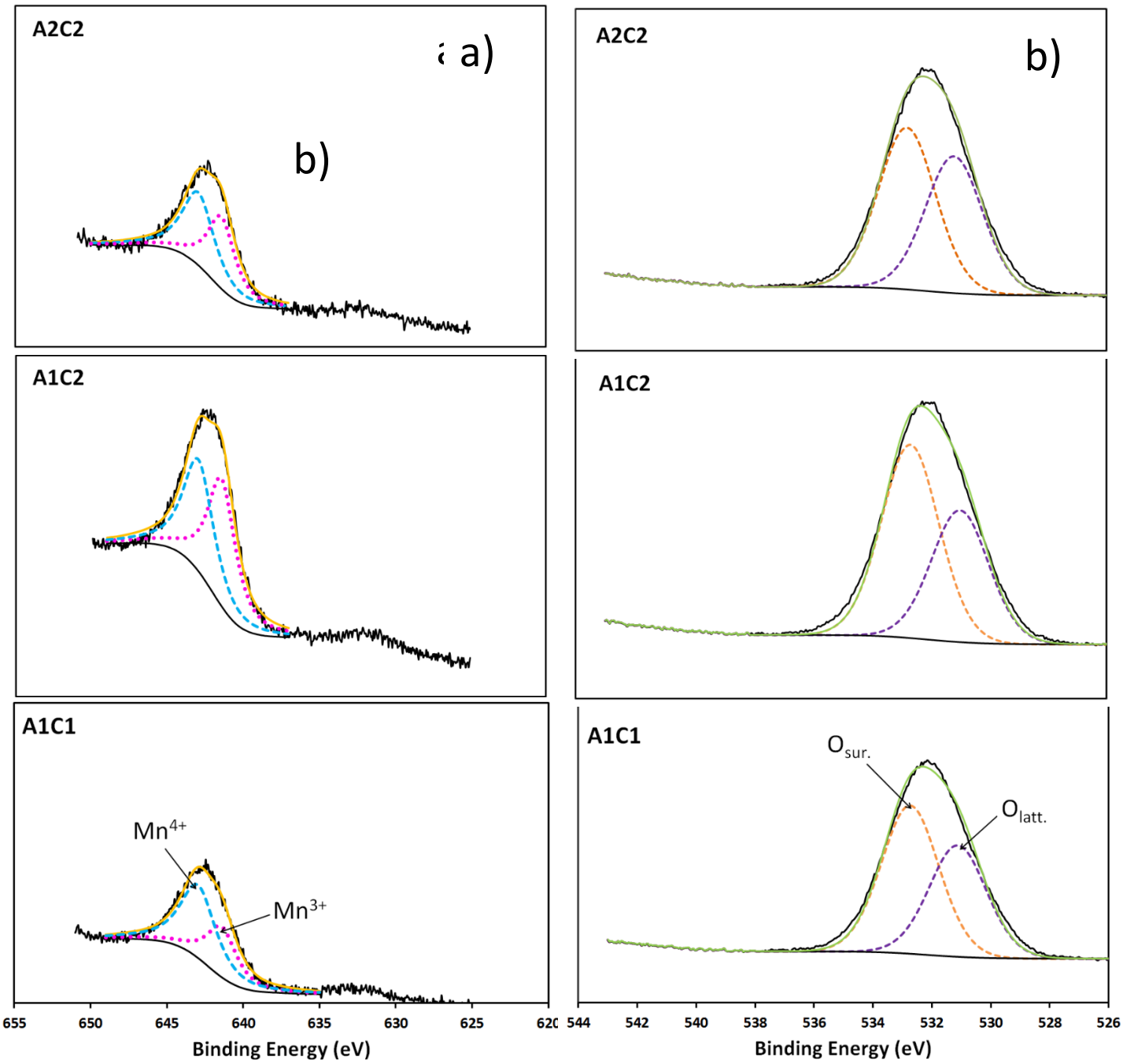

A2C2
a)
b)
A2C2
b)
A1C2
A1C2
A1C1
Mn4+
Mn3+
A1C1
Osur.
Olatt.
655
650
645
640
635
630
625
620
Binding Energy (eV)
544
542
540
538
536
534
532
530
528
526
Binding Energy (eV)

Figure 5

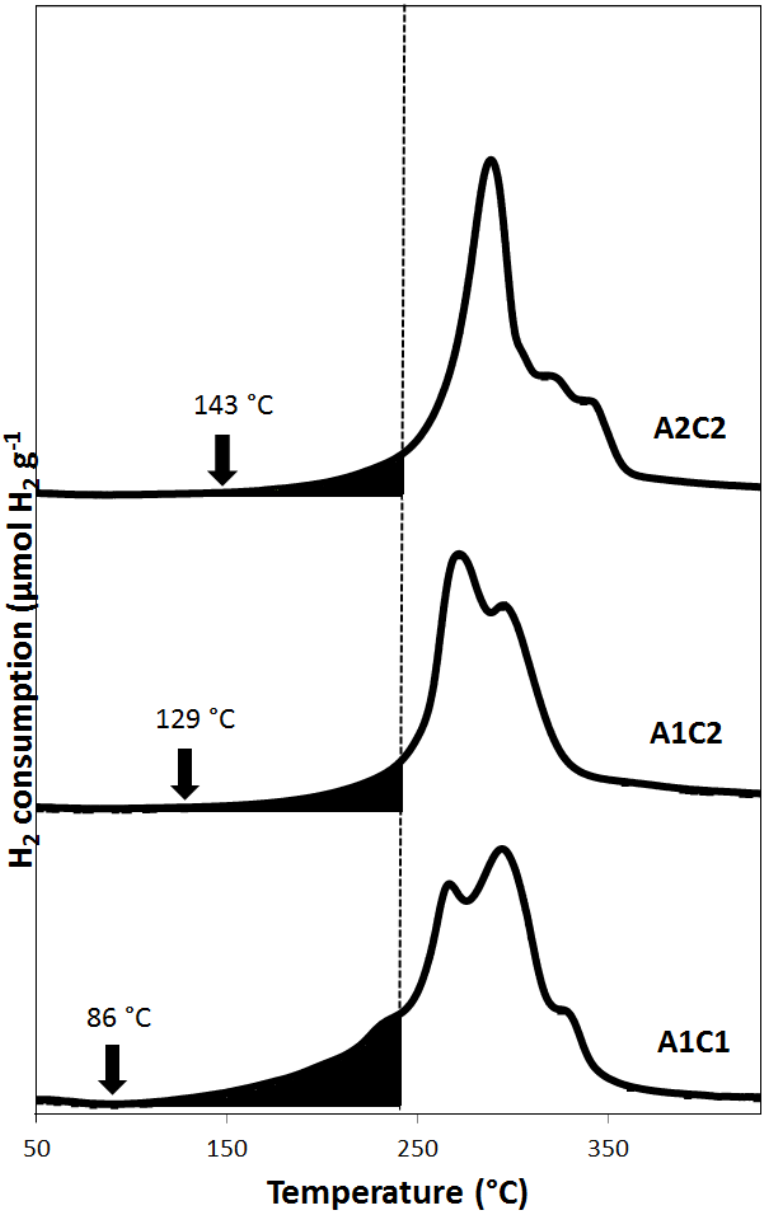

143 °C
A2C2
129 °C
A1C2
86 °C
A1C1
H2 consumption (µmol H2 g-1
50
150
250
350
Temperature (°C)

Figure 6

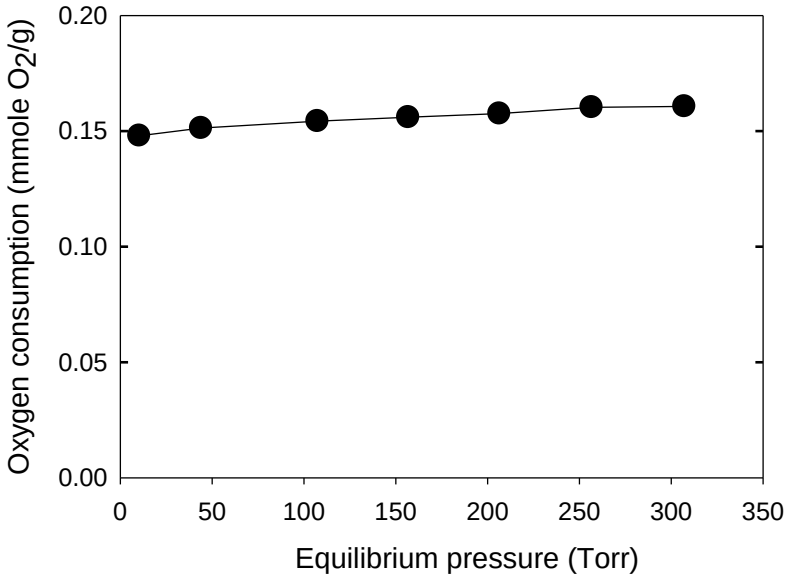

Oxygen consumption (mmole O_2/g)
0.20
0.15
0.10
0.05
0.00
0
50
100
150
200
250
300
350
Equilibrium pressure (Torr)

Figure 7

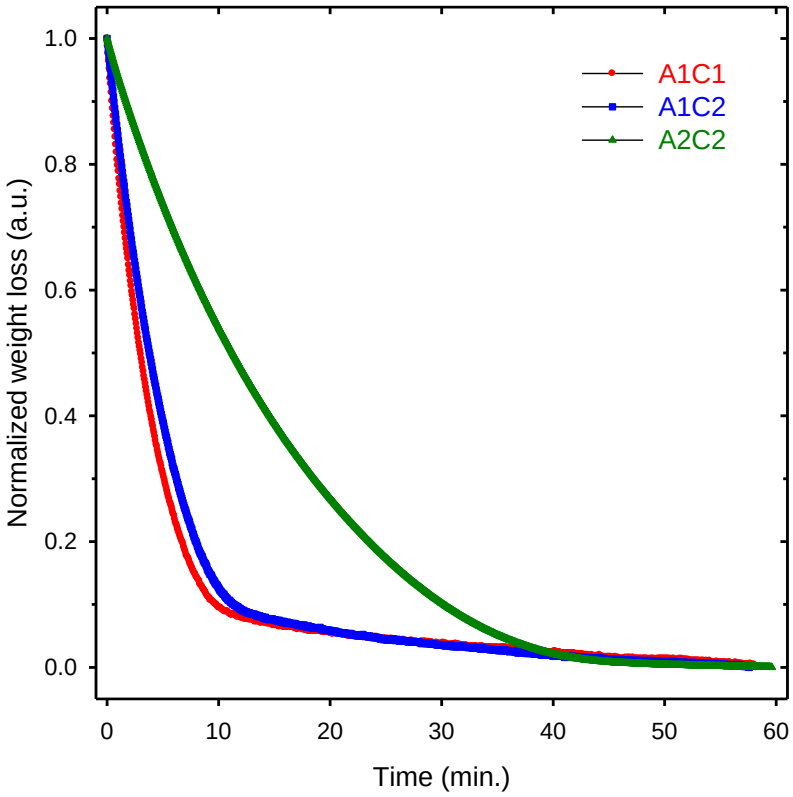

A1C1
A1C2
A2C2
Normalized weight loss (a.u.)
Time (min.)
0.0
0.2
0.4
0.6
0.8
1.0
0
10
20
30
40
50
60

Figure 8

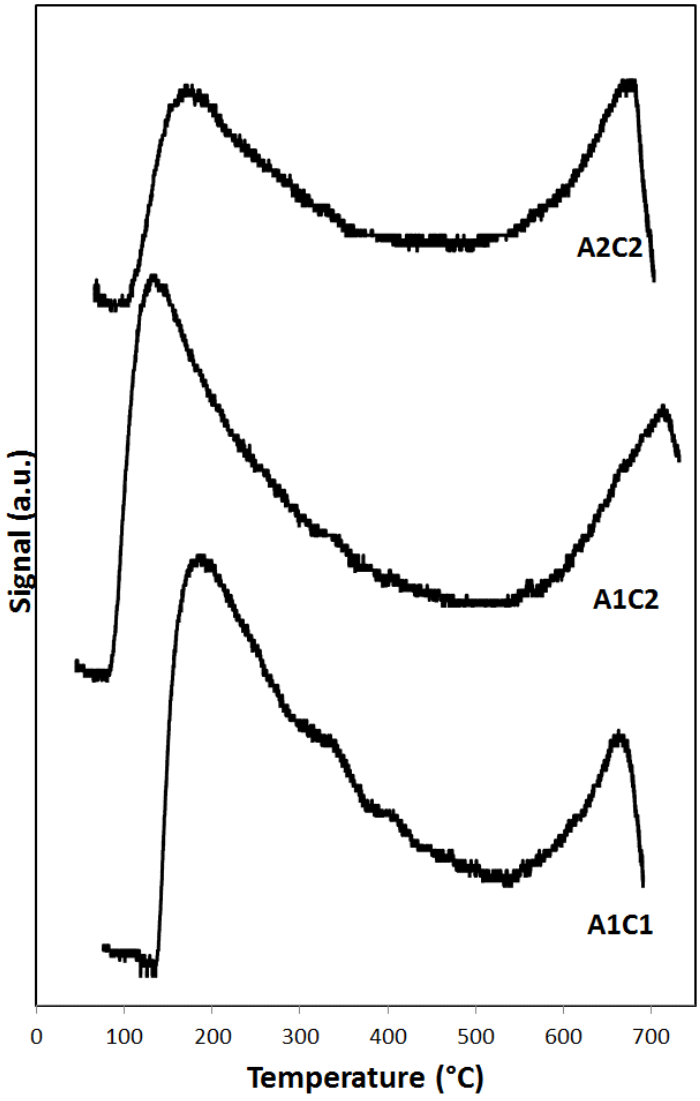
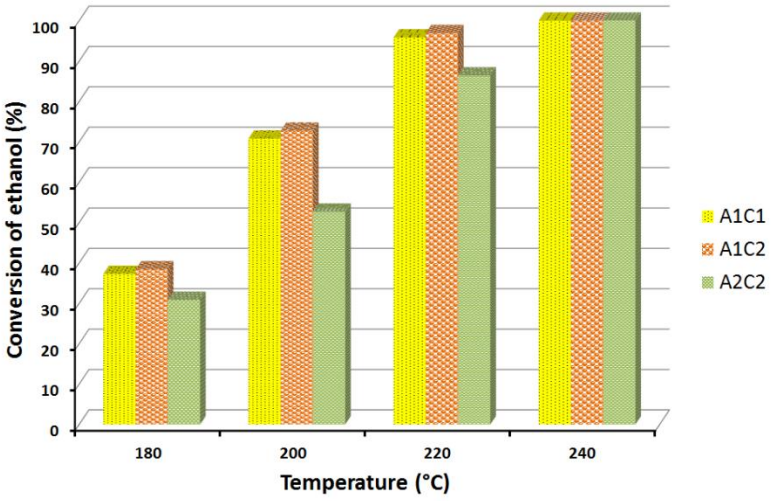
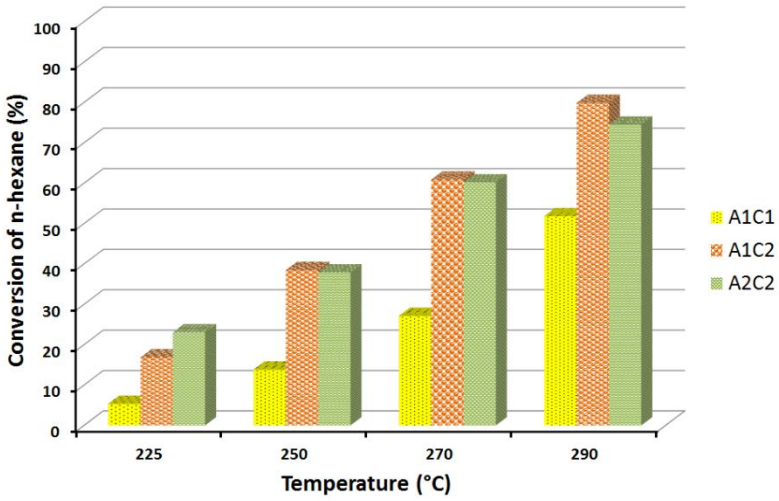
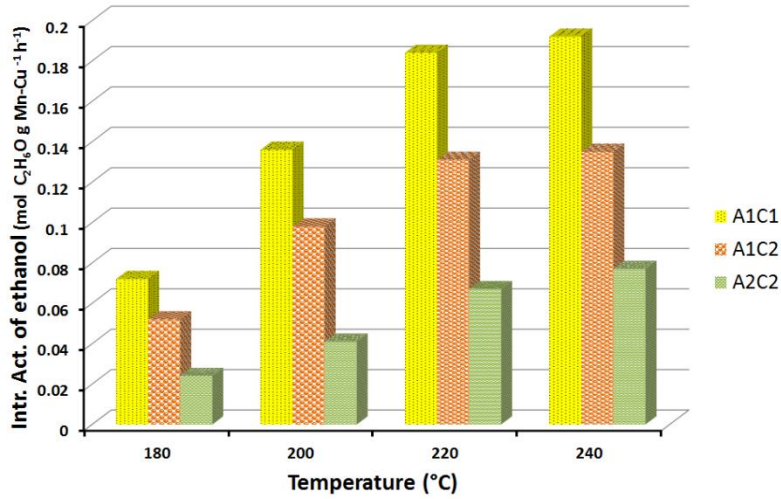

A2C2
A1C2
A1C1
Signal (a.u.)
0
100
200
300
400
500
600
700
Temperature (°C)

Figure 9


Conversion of ethanol (%)
100
90
80
70
60
50
40
30
20
10
0
180
200
220
240
Temperature (°C)
A1C1
A1C2
A2C2


Conversion of n-hexane (%)
100
90
80
70
60
50
40
30
20
10
0
225
250
270
290
Temperature (°C)
A1C1
A1C2
A2C2


Intr. Act. of ethanol (mol C2H6O g Mn-Cu-1 h-1)
0.2
0.18
0.16
0.14
0.12
0.1
0.08
0.06
0.04
0.02
0
180
200
220
240
Temperature (°C)
A1C1
A1C2
A2C2

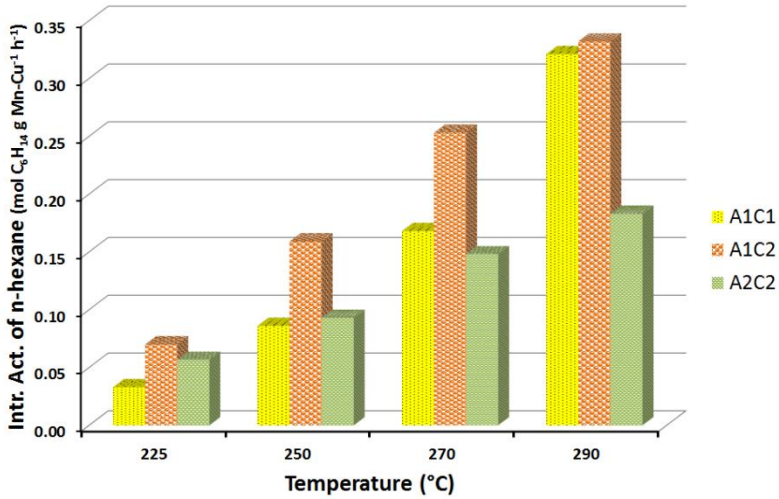
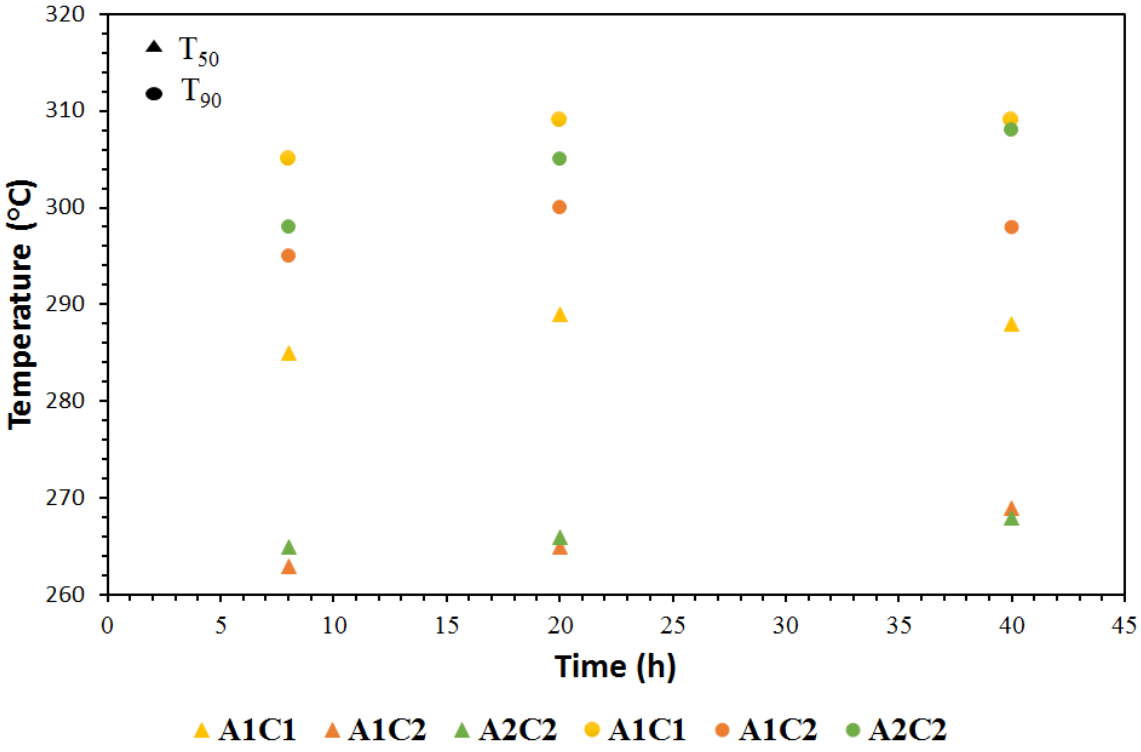

Intr. Act. of n-hexane (mol C6H14 g Mn-Cu-1 h-1)
0.35
0.30
0.25
0.20
0.15
0.10
0.05
0.00
225
250
270
290
Temperature (°C)
A1C1
A1C2
A2C2

Figure 10


T50
T90
Temperature (°C)
320
310
300
290
280
270
260
0
5
10
15
20
25
30
35
40
45
Time (h)
A1C1
A1C2
A2C2
A1C1
A1C2
A2C2

Supplementary Material

Click here to download Supplementary Material: Supplementary Material.docx